Carbohydrate Polymers 101 (2014) 631–641

Contents lists available at ScienceDirect

Carbohydrate Polymers

journal homepage: www.elsevier.com/locate/carbpol

A heteropolysaccharide, L-fuco-D-manno-1,6-α-D-galactan extracted from *Grifola frondosa* and antiangiogenic activity of its sulfated derivative

Ying Wang[a,1], Xiaokun Shen[b,c,1], Wenfeng Liao[a], Jianping Fang[a], Xia Chen[a], Qun Dong[a], Kan Ding[a,*]

[a] Glycochemistry and Glycobiology Lab, Shanghai Institute of Materia Medica, Chinese Academy of Sciences, Shanghai 201203, China
[b] Department of Oncology, Taizhou Hospital, Wenzhou Medical College, Linhai 317000, China
[c] Department of Medicine, Zhejiang University, Hangzhou 310029, China

ARTICLE INFO

Article history:
Received 28 March 2013
Received in revised form
22 September 2013
Accepted 24 September 2013
Available online 4 October 2013

Keywords:
Grifola frondosa
Galactan
Antiangiogenesis
Human microvascular endothelial cell line-1 (HMEC-1)

ABSTRACT

The tumor growth and metastasis are angiogenesis dependent, thus blockade of angiogenesis is a promising approach for treatment of cancer. Herein we reported the structural and biological features of a novel water-soluble polysaccharide named GFPW from the fruit body of *Grifola frondosa*. Chemical and spectral analysis revealed that GFPW with an average molecular weight of 15.7 kDa, possessed a backbone consisting of α-1,6-linked galactopyranosyl residues, with branches attached to O-2 of α-1,3-linked fucose residues and α-terminal mannose. By the chlorosulfonic acid–pyridine method, we prepared a sulfated derivative of GFPW, Sul-GFPW, with a substitution degree of 0.33. According to the ^{13}C NMR spectrum, the substitution position was deduced at C-2 and C-3. The angiogenesis assays *in vitro* showed that Sul-GFPW significantly inhibited endothelial cell proliferation in a dose- and time-dependent manner, and reduced endothelial cell migration and tube formation as well.

1. Introduction

Abnormal angiogenesis turns out to be a cause or consequence of numerous human diseases such as retinopathy, arthritis, endometriosis, ischemia and cancer (Azzam, 2007; Carmeliet, 2003). It is well established that blood vessels in tumor grow more rapidly than those in normal tissues and angiogenesis is required for tumor growth and metastasis. The angiogenesis is a complex process constituted by multiple steps. It actually starts with cancerous cells releasing molecules that activate endothelial cells to release enzymes to degrade the basement membrane. Endothelial cells then migrate and proliferate toward the source of the angiogenic stimulus, leading to the formation of solid endothelial cell sprouts into the stromal space. These sprouts then form loops to enable new vessels to grow across gaps in the vasculature. Consequently, blockade of angiogenesis has become an attractive approach for the treatment of some diseases especially for cancer (Shen et al., 2011). A number of small molecules have been developed as anti-angiogenic agents and several of them are currently undergoing clinical testing (Cole & Jayson, 2008). Evidences obtained recently have indicated that some polysaccharides and their sulfated derivatives such as laminarin sulfate were also potent angiogenesis inhibitors. The advantage of polysaccharides in this aspect should be that they can be designed to target several angiogenic molecules and they have lower side effect (Cole & Jayson, 2008; Hoffman, Paper, Donaldson, & Vogl, 1996; Kannagi, Izawa, Koike, Miyazaki, & Kimura, 2004; Lee et al., 2008). Therefore, saccharides may represent a novel class of antiangiogenic molecules and potentially provide therapeutic options for cancer.

Grifola frondosa (Fr.) S.F. Gray (Basidiomycetes, Aphyllopherales, Polyporaceae) is an edible and medicinal fungus used for centuries in Korea, Japan and China, which is commonly known by its nice almondy flavor and multiple medicinal properties. The dry fruit body of *G. frondosa* is generally marketed as health foods, including teas, whole powders, granules, drinks, and tablets (Kubo, Aoki, & Nanba, 1994; Masuda, Inoue, Miyata, Mizuno, & Nanba, 2009; Ulbricht et al., 2009). The medicinal properties of *G. frondosa* have been studied since the mid-1980s (Ohno et al., 1984). The extracts from fruiting body or liquid cultured mycelium of *G. frondosa* contain carbohydrates, proteins, peptides and lectins. These different

* Corresponding author at: 555 Zu Chong Zhi Road, Pudong, Shanghai 201203, China. Tel.: +86 21 50806928; fax: +86 21 50806928.
E-mail address: dingkan@simm.ac.cn (K. Ding).
[1] These authors contributed equally to this work.

0144-8617/$ – see front matter © 2013 Elsevier Ltd. All rights reserved.
http://dx.doi.org/10.1016/j.carbpol.2013.09.085

ingredients were thought to be responsible for the different biological activities such as antitumor, anti-mutagenic, antihypertensive, anti-diabetic, hypolipidemic, antioxidant, antiviral, and stimulation of collagen biosynthesis (Cui et al., 2007; Kubo & Nanba, 1997; Shih, Chou, Chen, Wu, & Hsieh, 2008; Shomori, Yamamoto, Arifuku, Teramachi, & Ito, 2009). Among them, MD-fraction isolated from the fruiting body has been extensively investigated. MD-fraction is a glucan with β-1,6-linked main chain and very frequently, to which β-1,3-linked branches are attached. This fraction showed antitumor effects by activating host immune defense and thus inhibiting of tumor cell proliferation (Kodama et al., 2005; Masuda, Murata, Hayashi, & Nanba, 2008; Ohno, Asada, Adachi, & Yadomae, 1995). In this report, we isolate a polysaccharide designated GFPW, from the fruit body of *G. frondosa*. To our knowledge, GFPW has the characteristic structure that has not been reported previously. In addition, we also investigated the effects of GFPW and its sulfated derivative Sul-GFPW on angiogenesis *in vitro*.

2. Materials and methods

2.1. Materials

The dried fruit bodies of *G. frondosa* were purchased from the local market (Dashahe, Shanghai, China). DEAE-cellulose 32 was from Whatman. Sephacryl S-300 HR was from Pharmacia Biotech. Bio-Gel P-2 was from Bio-Rad. Standard monosaccharides, sodium borohydride and iodomethane were all Fluka products. 3-(4,5-Methylthiazol-2-yl)-2,5-diphenyl-tetrazolium bromide (MTT) was from Sigma–Aldrich. Dimethyl sulfoxide (DMSO) was from Merck. Matrigel for tube formation assay with growth factor was from BD (BD Biosciences, USA). All the reagents used were of analytical grade unless otherwise claimed.

2.2. General methods

All evaporations were carried out at 45 °C under reduced pressure. IR spectra were determined with a Perkin-Elmer 591B spectrophotometer as KBr pellets (native polysaccharides) or Nujol films (permethylated polysaccharides). Optical rotations were determined with a Perkin-Elmer 241M digital polarimeter. High performance gel permeation chromatography (HPGPG) was performed with a Waters instrument, including a 515 HPLC pump, a 2410 RI detector and a 2487 dural UV absorbance detecot and GPC software (Waters, Millennium^{32}, 1998). NMR spectra were recorded on a Varian Mercury 400 NMR spectrometer. DEPT experiments were carried out using a polarization transfer pulse of 135. Gas chromatography (GC) was conducted on a Shimadzu GC-14B instrument, equipped with a 3% OV-225-packed glass column (3.2 mm × 200 cm) and an FID detector. The column temperature was kept at 210 °C for sugar analysis, and the carrier gas was N_2 at flow rate of 25 mL/min. The injection and detection temperatures were at 250 °C and 240 °C, respectively. GC–MS was performed with a Shimadzu QP-5050A apparatus equipped with a DB-1 capillary column (0.25 mm × 30 m). Electrospray ionization mass spectrometry (ESI-MS) spectra were measured with a VG Quattro MS/MS spectrometer.

2.3. Isolation and purification of GFPW

The fruit bodies of *G. frondosa* (3 kg), defatted with 95% EtOH for 7 days each time, repeated twice. The defatted residue was extracted with boiling water for four times (6 h each time). The aqueous extract was concentrated and deproteinated with 15% trichloroacetic acid at 4 °C to remove protein. After neutralization and centrifugation, the supernatant solution was intensively dialyzed against running water (molecular weight cut-off 3500 Da) for 2 days, and then concentrated to small volume. Three volumes of 95% EtOH were added to the concentrated retentate slowly to precipitate the crude polysaccharide (150 g, yield 5%). A portion of the crude polysaccharide fraction named GFP (10 g) was loaded onto a DEAE-cellulose column (6 cm × 80 cm), eluted with distilled water and monitored with a phenol–sulfuric acid. Then this fraction was further purified on a column of Sephacryl S-300 HR (2.6 cm × 100 cm) which was equilibrated and eluted with distilled water to give one major fraction, GFPW (280 mg, yield 2.8%), monitored with phenol-sulfuric acid method.

2.4. Homogeneity and molecular weight

The homogeneity and molecular weight of polysaccharide were estimated by HPGPC with TSK G3000 column (Dodgson & Price, 1962), eluted with mobile phase containing 0.4 g/L KH_2PO_4 and 7.32 g/L K_2HPO_4 at a flow rate of 0.5 mL/min. The column temperature was kept at 30 ± 0.1 °C. For molecular weight estimation, the column was calibrated by standard Dextrans (T-700, T-580, T-110, T-80, T-40, T-11, Pharmacia). Data were processed by GPC software. All samples were prepared as 0.2% (w/v) solution, and 20 μL of solution was analyzed in each run.

2.5. Monosaccharide composition analysis

The polysaccharide (2 mg) was hydrolyzed in 2 M trifluoroacetic acid (TFA, 2 mL) at 110 °C for 2 h in a sealed test tube. After evaporation to completely remove TFA, the residue was dissolved in water (0.2 mL). 5 μL of the solution was used for TLC analysis. The other hydrolysate was dissolved in distilled water (2 mL) and reduced with $NaBH_4$ (30 mg) for 3 h. After neutralization with AcOH and evaporation to dryness, the residue was acetylated with Ac_2O at 100 °C for 1 h, and converted into the alditol acetates, followed by GC analysis.

2.6. NMR and MS analysis

A polysaccharide sample (40 mg) was exchanged by D_2O, and then dissolved in 0.5 mL of D_2O (99.8% D). The ^1H, ^{13}C NMR spectra, heteronuclear single quantum coherence (HSQC), and heteronuclear multiple bond correlation (HMBC) spectra were measured at 25 °C with acetone as internal standard (31.50 ppm for carbon). All chemical shifts were in reference to Me_4Si. The distortionless enhancement by polarization transfer (DEPT) experiment was done using a polarization-transfer pulse of 135°. For ESI-MS the carbohydrates were dissolved in MeOH/H_2O (1:1, v/v).

2.7. Methylation composition analysis

Methylation of GFPW was carried out using the method of Needs and Selvendran (1993) with minor modifications as described previously (Xu, Dong, Qiu, Cong, & Ding, 2010). Briefly, 10 mg of dry GFPW was weighed precisely and dissolved in 2 mL of DMSO before 20 mg NaOH was added. The mixture was then treated with an ultrasonic wave for 5 min. And then put the reaction bottle into ice water. Methyl iodide (0.3 mL) was added in 15 min. The sample was kept for 30 min before 2 mL distilled water added to stop the reaction. The methylated polysaccharides were dialyzed against water for 24 h followed by concentration to a small volume. The sample was extracted with 1 volume of chloroform for 3 times, dried by Na_2SO_4 and then evaporated by N_2.

2.8. Partial acid hydrolysis

GFPW (100 mg) was first hydrolyzed in 0.1 M TFA (20 mL) and incubated at 100 °C for 1 h. After cooling, concentration, and

dialysis, the retentate was lyophilized, giving GFPW-De1, followed analysis by HPGPC. GFPW-De1 was further hydrolyzed with 0.2 M TFA (20 mL) and kept at 100 °C for 2 h, then evaporated to dryness and dialyzed for 24 h. The nondialysate was freeze-dried, giving GFPW-De2, then monosaccharide composition analysis, HPGPC and ^{13}C NMR analysis were performed for the polysaccharide. The concentrated dialysate giving GFPW-De2-O, was applied to a Bio-Gel-P2 column (1.6 cm × 100 cm) and eluted with water, and was separated into four fractions, GFPW-I, De2-O3, De2-O2 and De2-O1. Each fraction was subjected to composition analysis, ESI-MS or ^{13}C NMR analysis, respectively.

2.9. Acetolysis analysis

Acetolysis analysis was performed as previously described (Bao, Fang, & Li, 2001). GFPW (100 mg) was treated with a 10:10:1 (v/v/v) mixture of HAc–Ac_2O (acetic acid–acetic anhydride)-concentrated H_2SO_4 at 40 °C for 8 h (Vaishnav, Bacon, O'Neill, & Cherniak, 1998). The acetolysate was de-O-acetylated with 0.2 M sodium methoxide (NaOAc) in methanol (MeOH), and the solution was passed through 732# (H^+) cation exchange column. The pooled eluent was loaded onto a Bio-Gel-P2 column (1.6 cm × 100 cm) eluted with water and different carbohydrate fractions were pooled and lyophilized.

2.10. Preparation of sulfated polysaccharide derivative

Sulfated derivative of GFPW was prepared by the chlorosulfonic acid–pyridine method (Inoue, Kohno, & Kadoya, 1983) at 45 °C for 4 h, using formamide as the solvent. The ratio of chlorosulfonic acid and pyridine was 1:2 (v/v). After the reaction, the pH of the solvent was adjusted to pH 7.8 and then dialyzed against 2 L supersaturated $NaHCO_3$ overnight. The solvent was lyophilized after dialyzing against 2 L deionized water for three times.

2.11. Cell culture

Human microvascular endothelial cells (HMEC-1) were maintained in MCDB131 (Gibco BRL, USA) medium containing 15% FBS (*v/v*), 2 mM L-glutamine, 10 ng/mL EGF (Shanghai PrimeGene Bio-Tech Co. Ltd., Shanghai, China) and antibiotics (100 U/mL penicillin, 100 μg/mL streptomycin (Gibco BRL, USA)) in a humidified 5% CO_2 incubator at 37 °C.

2.12. MTT assay

MTT analysis was performed as previously described (Chen et al., 2011). To evaluate the cell proliferation, HMEC-1 cells were seeded at a density of 2×10^3 cells/well into a sterile 96-well plate and grown in 5% CO_2 at 37 °C for 24 h. GFPW and Sul-GFPW were dissolved in PBS and diluted with culture medium into different concentrations. After treatment with the polysaccharides, HMEC-1 cell viability was measured by 3-(4,5-dimethylthiazol-2-yl)-2,5-diphenyltetrazolium bromide (MTT; Sigma–Aldrich) assay. A solution of 5 mg/mL MTT was then added to each well and incubated with HMEC-1 cells for another 4 h in the incubator. After the medium was removed, the formazan was solubilized in 150 μL DMSO. And then the optical density was measured using a spectrophotometer (Thermo Multiskan MK3, Germany) at an absorption wavelength of 570 nm. The inhibition rate was calculated as [(control − sample)/control] × 100%. Each experiment was performed in triplicate.

2.13. Cell cycle analysis

Cell cycle phase was assayed by DNA fragment staining using PI (propidium iodide). Cells (1×10^6/well) were plated into a 6-well plate for 24 h, followed by treatment with or without 100 μg/mL of Sul-GFPW for 24 h. Then cells were harvested and centrifuged (3000 rpm, 5 min), cells were suspended to a density of 1×10^6 cells/mL after washing twice with PBS. The cells were fixed and permeabilized by adding 70% ethanol (1 mL/tube) for more than 2 h at −20 °C. After centrifugation, the ethanol were decanted and cell pellets were suspended in 0.5 mL of staining solution containing 200 μL of DNase-free RNase and 200 μL of PI, followed by incubation for 30 min at room temperature in dark. The cells were immediately subject to flow cytometry analysis. Cell cycle was analyzed using BD FACScalibur flow cytometer. The percentage of cells stained by propidium iodide was calculated using ModFit LT software. Experiments were repeated thrice. The column showed the percentage of cell distribution in each cell phase as mean ± SD ($n = 3$).

2.14. Scratch wound healing assay

The scratch wound healing assay was performed as previously described (Qiu, Yang, Pei, Zhang, & Ding, 2010). Briefly, HMEC-1 cells (5×10^5) were cultured in 6-well plates for 24 h. Confluent cell monolayers were scraped with a yellow pipette tip to generate a wound and rinsed twice with growth medium, followed by treatment with or without 100 μg/mL of Sul-GFPW for 36 h. An anti-angiogenesis sulfated polysaccharide, WSS25 (25 μg/mL) was employed as positive control (Qiu, Yang, Pei, Zhang, & Ding, 2010). The cells were photographed immediately after the scratch and 36 h later with an Olympus IX 51 digital microscope.

2.15. Tube formation assay

The tube formation assay was performed to determine the effect of sulfated derivative of GFPW (Sul-GFPW) on angiogenesis *in vitro*. In this experiments, WSS25 (25 μg/mL) was also employed as a positive control. Briefly, a 96-well plate coated with 50 μL of matrigel per well was allowed to be solidified at 37 °C for 30 min. HMEC-1 cells (3×10^4/well) were seeded into the plate and cultured in MCDB131 media containing 100 μg/mL of Sul-GFPW or 25 μg/mL of WSS25 for 8 h. The enclosed capillary networks of tubes were photographed under a microscope (Olympus IX 51, Japan).

2.16. Statistical analysis

Statistical analyses were performed using Student's *t*-test. Significant difference between two groups was defined as $p < 0.05$ ($^*p < 0.05$; $^{**}p < 0.01$).

3. Results and discussion

3.1. Isolation and monosaccharide composition analysis of GFPW

GFPW was isolated by anion-exchange chromatography on a DEAE-cellulose column eluted with water from the crude polysaccharide extracted from *G. frondosa* fruit body (5.26% of the crude polysaccharide GFP) with boiling water, and purified by repeated gel permeation chromatography on a column of Sephacryl S-300 eluted with water. The homogeneity of GFPW was estimated by HPGPC, which showed one symmetrical peak. The molecular weight (*MW*) of GFPW was estimated to be 1.57×10^4 Da, and its specific rotation [α] was +72 (*c* 0.5, H_2O). There was no absorption peak at 280 nm in UV (ultraviolet) spectrum of GFPW. Lowry assay of GFPW showed a negative response (Nakajima et al., 1983), indicating that it was free of protein. After complete hydrolysis with 2 M TFA, GFPW was shown by thin layer chromatography (TLC) to contain no uronic acid. Monosaccharide composition analysis

Table 1
GC–MS data for methylation analysis of polysaccharide GFPW.

Methylated sugars	Linkages	Molar percent (%)	Mass fragments (*m*/*z*)
2,4-Me_2-Fuc*p*	1,3-	21.96	117, 131, 89, 173, 201, 233
2,3,4,6-Me_4-Man*p*	Terminal	19.49	101, 129, 161, 205, 71
2,3,4-Me_3-Gal*p*	1,6-	28.56	101, 117, 129, 87, 161, 189, 233
3,4-Me_2-Gal*p*	1,2,6-	19.71	129, 87, 189, 87, 43, 233

showed GFPW contained mannose, fucose and galactose in ratio of 0.41:0.44:1.

3.2. Linkage analysis of GFPW

In order to determine the glycosyl linkage types, GFPW was subjected to methylation analysis. The methylation results were analysis by comparing the standard figure and combining with monosaccharide ratio (Miao, Li, Shen, Wang, & Jiang, 2011; Qiu, Yang, Pei, Zhang, & Ding, 2010; Xu, Dong, Qiu, Cong, & Ding, 2010). We deduced that the intrachain residues were probably 1,3-linked Fuc*p* (21.96%) and 1,6-linked Gal*p* (28.56%). The non-reducing terminals consisted of T-Man*p* (19.49%), indicating that GFPW was significantly branched. The main branching points were supposed to be at 1,2,6-linked Gal*p* (19.71%) (Table 1). The ratio of T-Man*p*, 1,3-linked Fuc*p*, 1,6/1,2,6-linked Gal*p* was 0.40:0.45:1. This was consistent with the ratio of monosaccharide in the results of monosaccharide composition analysis.

3.3. Partial acid analysis

To determine the detailed structure features, GFPW (100 mg) was partially hydrolyzed with 0.1 M TFA and the hydrolysate was dialyzed, giving GFPW-De1 (nondialysate, 65 mg). The data of HPGPC result showed GFPW-De1 was also homogenous and its *MW* was 1.5×10^4 Da. Monosaccharide analysis showed that it was composed of Fuc, Man, Gal, in a molar ratio of 0.35:0.41:1. In this case, GFPW had not been degraded significantly. Then GFPW-De1 (65 mg) was further degraded in 0.2 M TFA at 100 °C for 2 h, giving GFPW-De2 (nondialysate, 37 mg) and GFPW-De2-O (dialysate). GFPW-De2-O was subjected to Bio-Gel-P2 eluted by water, which was separated into four fractions, GFPW-I (6.3 mg), De2-O3 (8.6 mg), De2-O2 (3.6 mg) and De2-O1 (2.3 mg).

The degraded polysaccharide GFPW-De2 was mainly composed of Gal, with a *MW* of 9.0×10^3 Da indicating that almost all of the Fucopyranosyl residues and mannopryanosyl residues were released as monosaccharides or oligosaccharides upon the hydrolysis. So it was deduced that the main chain of GFPW-De2 may be a galactan which was confirmed by its ^{13}C NMR spectrum (Fig. 1A). There was only one signal in anomeric carbon area, the signal at 100.3 ppm was attributed to C1 of Gal*p*, while the signal at 68.879 ppm was assigned to C-6 of 1,6-linked Gal*p* (Cui et al., 2008). Hence the results suggested GFPW-De2 was a (1→6)-linked galactan.

Comparing with the elution volume of the standard samples (Blue Dextran T-2000, maltose, fucose and mannose) on Bio-Gel-P2, GFPW-I was in the exclusive volume (data not shown), which was not analysis further. De2-O3 was designated to disaccharide according to its retention volume with standard oligosaccharide on Bio-Gel-P2. The ESI-MS spectrum (Fig. 1B) of De2-O3 showed a main molecular ion at *m*/*z* 349 $[M+Na]^+$ that correspond to a disaccharide composed of one hexosyl and de-O-hexosyl residues. The monosaccharide composition analysis showed that De2-O3 was composed of Fuc and Man. The molar ratio of Fuc and Man was about 1.4:1. Interestingly, we found that fucose and mannose could be separated by Bio-Gel-P2 eluted with water (data not shown). The monosaccharide composition analysis showed that De2-O1 mainly contained mannose and De2-O2 mainly contained fucose. Hence, we deduced that De2-O1 and De2-O2 were designated to mannose and fucose monosaccharide, respectively, combined by their monosaccharide composition analysis results. Because De2-O3 is a disaccharide, composed of Fuc and Man. Meanwhile, De2-O2 was mainly composed of Fuc. In ^{13}C NMR of De2-O2, the signal at 97.38 ppm was corresponded to C1 of β-Fuc*p*, while 93.51 ppm was assigned to C1 of α-Fuc*p* of De2-O2 (Fig. 1C). Thus, the ^{13}C NMR of De2-O3 would be easily analyzed with the help of ^{13}C NMR of De2-O2. In ^{13}C NMR of De2-O3 (Fig. 1D), the signal at 97.38 ppm was corresponded to C1 of β-1,3-Fuc*p*, 93.51 ppm was to C1 of α-1,3-Fuc*p*. The signal at 102.79 ppm was assigned to the anomeric carbon of T-Man*p*. We deduced that 1,3-linked Fuc*p* was at the reducing end, the anomeric carbon would influence the signal of C-3 of Fuc*p*, both the signal at 81.23 ppm and 77.37 ppm were assigned to C-3 of 1,3-linked Fuc*p* (Fig. 1D) (Bock, Pedersen, & Pedersen, 1984). The signal at 17.42 ppm was from C6 of CH_3-Fuc*p*. These results indicated that De2-O3 contained a disaccharide as T-Man*p*-(1→3)-Fuc*p*-1-α/β.

3.4. Acetolysis analysis

To confirm the detailed structure features, GFPW was treated with acetolysis analysis. The acetolysis product was subjected to Bio-Gel-P2. There was nearly no polysaccharide being tested (data not shown) in the exclusive volume. This meant the polysaccharide was cleaved completely. Since acetolysis will take advantage of the selective cleavage of 1,6-linked residues (Bao, Fang, & Li, 2001), the results reconfirmed that the back bone of GFPW is a α-(1→6)-galactan, which was consisted with the above results suggested.

3.5. NMR analysis

In the ^{13}C NMR spectrum of GFPW (Fig. 2A), the signal of Gal of GFPW was easily be assigned combined by the ^{13}C NMR spectrum of GFPW-De2 (Fig. 1A). The signal of 99.18 ppm was corresponded to 1,6-linked and 1,2,6-linked Gal*p* (Ye et al., 2008). The resonance signals of Man and Fuc of GFPW were assigned by reference to the ^{13}C NMR spectrum of GFPW-De2-O2 (Fig. 1C) and GFPW-De2-O3 (Fig. 1D) described in the above analysis. The signal at 103.51 ppm was assigned to the anomeric carbon of Man (Molinaro, Piscopo, Lanzetta, & Parrilli, 2002), while the signal at the anomeric carbon area of 102.56 ppm corresponded to the non-reducing end of 1,3-linked Fuc*p* (Perepelov et al., 2007). The signal at 77.31 ppm was assigned to C-2 of 1,2,6-linked Gal*p* (Ye et al., 2008). The signal at 77.48 ppm was corresponded to C-3 of 1,3-linked Fuc*p*. The signal at 68.057 ppm was assigned to C-6 of 1,6-linked and 68.15 ppm was to 1,2,6-linked Gal*p* (Harding et al., 2005; Ye et al., 2008). The signal at 61.04 ppm was attributed to C-6 of T-Man*p*. The absence from the ^{13}C NMR spectrum of signals within 82–88 ppm region suggested that all sugar residues were in the pyranose form (Fan et al., 2006). ^{1}H NMR spectra of GFPW in Fig. 2B showed one broad anomeric signal at about 5.2 ppm and no signal at 4.6 ppm. The results confirmed the α-configuration of the glycan residues (Vinogradov & Wasser, 2005). The anomeric signals in the ^{1}H NMR spectrum of GFPW were assigned mainly according to the carbon and hydrogen correlations in the HSQC and HMBC spectra (Fig. 3). The signal

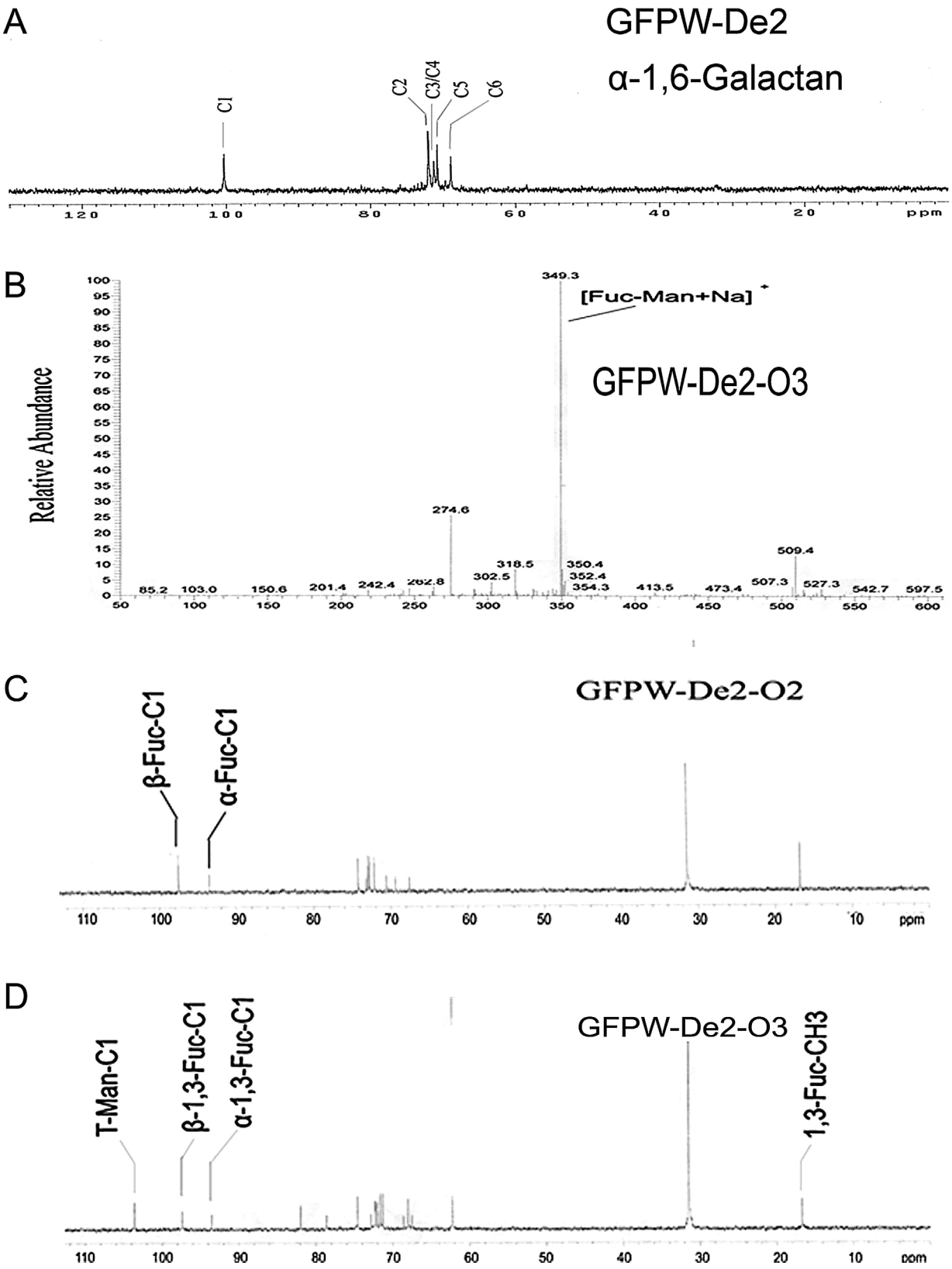

Fig. 1. NMR spectrum analysis of GFPW-De2, GFPW-De2-O2 and GFPW-De2-O3, ESI-MS spectrum of GFPW-De2-O3. (A) ^{13}C NMR spectrum of GFPW-De2. (B) ESI-MS spectrum of GFPW-De2-O3. (C) ^{13}C NMR spectrum of GFPW De2-O2. (D) ^{13}C NMR spectrum of GFPW De2-O3.

at 5.17 ppm was assigned to α-1,3-linked Fuc*p*, and the signal at 5.11 ppm was assigned to the non-reducing terminal α-Man*p*. The signal at 5.07 ppm originated from α-1,6-linked Gal*p* and/or α-1,2,6-linked Gal*p*. Other signals were assigned in reference to values found in the literature (Inoue, Nakajima, et al., 1983; Molinaro, Piscopo, Lanzetta, & Parrilli, 2002; Perepelov et al., 2007; Ye et al., 2008) or according to HSQC and HMBC (Fig. 3), and the results are shown in Table 2.

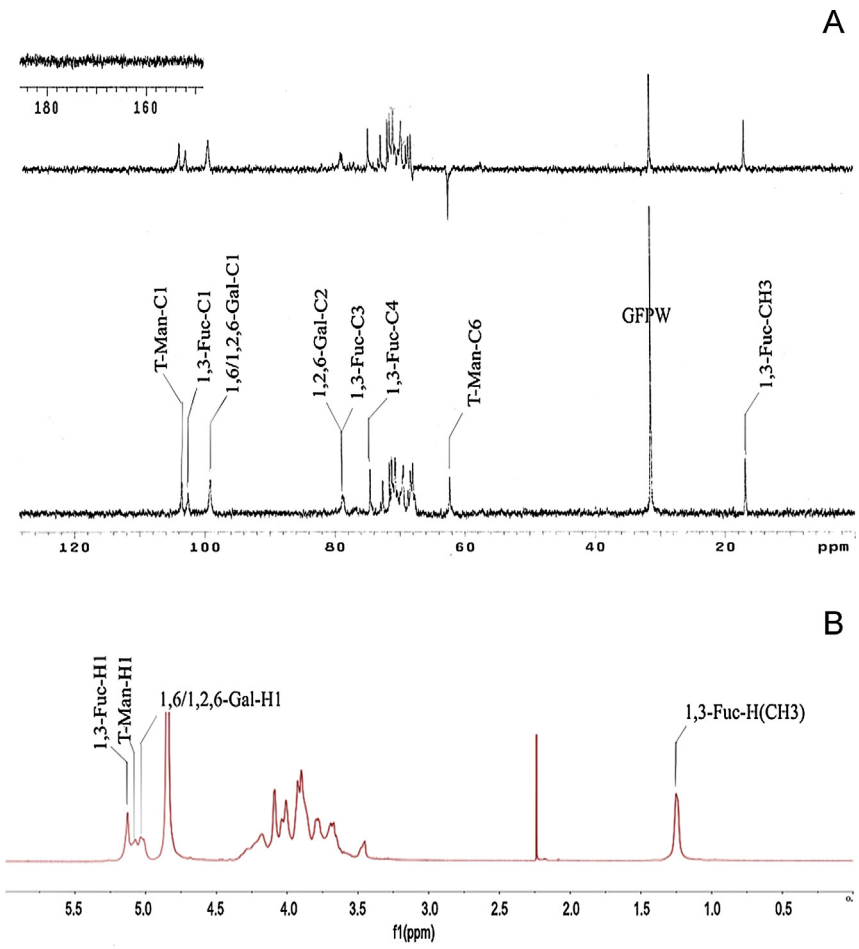

Fig. 2. NMR spectrum of GFPW. (A) ^{1}H NMR spectrum of GFPW. (B) ^{13}C NMR spectrum of GFPW.

Based on the above results, it could be concluded that the GFPW was a neutral polysaccharide having a α-1,6-linked Gal*p* backbone (28.56%). The non-reducing terminals consisted of Man*p* (19.49%) indicating that GFPW was significantly branched. The main branching point was at C-2 of α-1,2,6-linked Gal*p* (19.71%). Hence, we proposed a putative structure for GFPW as followed:

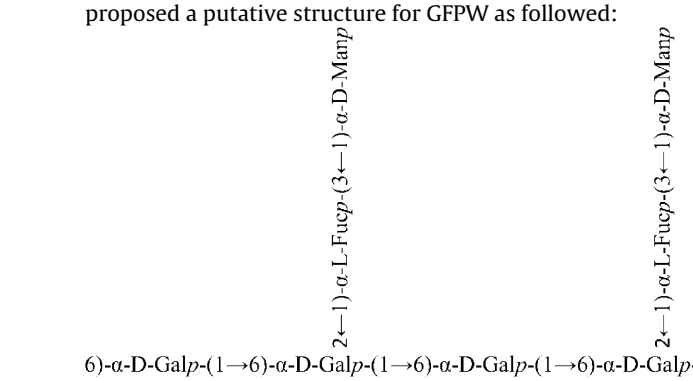

The structure was different from the reported structure of polysaccharide MD-fraction isolated from fruiting bodies of *G. frondosa*, which is a glucan with a β-1,6 main chain substituted with β-1,3 linked branches and trace protein.

3.6. Preparation of sulfated derivative from GFPW

A sulfated derivative named Sul-GPFW was prepared from GFPW by pyridine–chlorosulfonic acid method. A S—O—S signal near 827 cm^{-1} and a S═O signal near 1247 cm^{-1} in the IR spectrum were shown in Fig. 4A, indicating that Sul-GFPW was successfully sulfated. The degree of substitution (DS) of GFPW and Sul-GFPW were 0 and 0.33, respectively, and the results were shown in Table 3, as determined by the $BaCl_2$-gelatin method (Dodgson & Price, 1962).

GFPW may be subjected to partial degradation due to the lability of Fuc*p* and Man*p* residues to the acidic condition for sulfation. In the ^{13}C NMR spectrum of GFPW and Sul-GFPW (Fig. 4B), there was only one carbon signal in the anomeric carbon area, the carbon signal of mannose and fucose disappeared. The signal at 98.95 ppm was corresponded to C-1 of Gal*p*. The sulfated C-3 signal of Gal*p* appeared at 80.56 ppm, the signal at 74.92 ppm was assigned to the sulfated C-2 signal of Gal*p* (Held et al., 2011). The additional smaller C-3 signal of Gal*p* appeared at 76.99 ppm was caused by the sulfation at C-2 of Gal*p* (Xu, Dong, Qiu, Ma, & Ding,

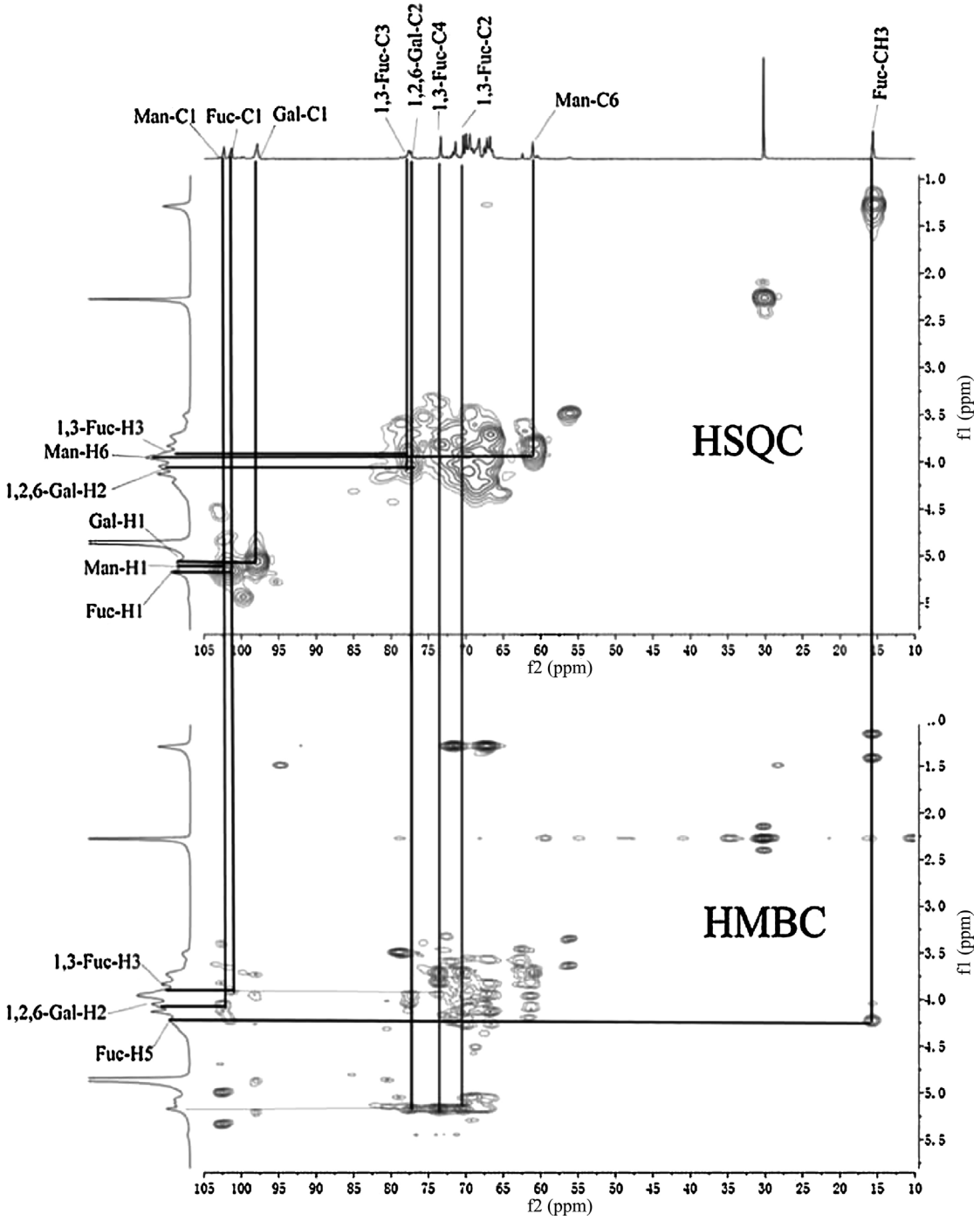

Fig. 3. HSQC and HMQC spectra of GFPW.

Table 2
^{1}H and ^{13}C NMR spectral assignments for GFPW.

Residues		1	2	3	4	5	6
T-α-Man	H	5.11	4.22	4.09	3.91	4.06	3.81 (3.93)[a]
	C	103.51	68.3	69.7	67.47	70.23	61.04
1,3-α-Fuc	H	5.17	3.98	3.91	3.96	4.27	1.15
	C	102.56	70.52	77.48	73.38	68.77	17.42
1,6-α-Gal	H	5.07	3.72	3.91	4.08	4.11	3.72 (3.95)[a]
	C	99.18	71.37	69.92	70.07	69.16	68.05
1,2,6-α-Gal	H	5.07	4.04	4.03	3.90	4.11	3.72 (3.95)[a]
	C	99.18	77.31	71.61	71.43	69.27	68.15

[a] The values inside and outside the brackets denote the chemical shifts of H-6 at axial and equatorial positions, respectively.

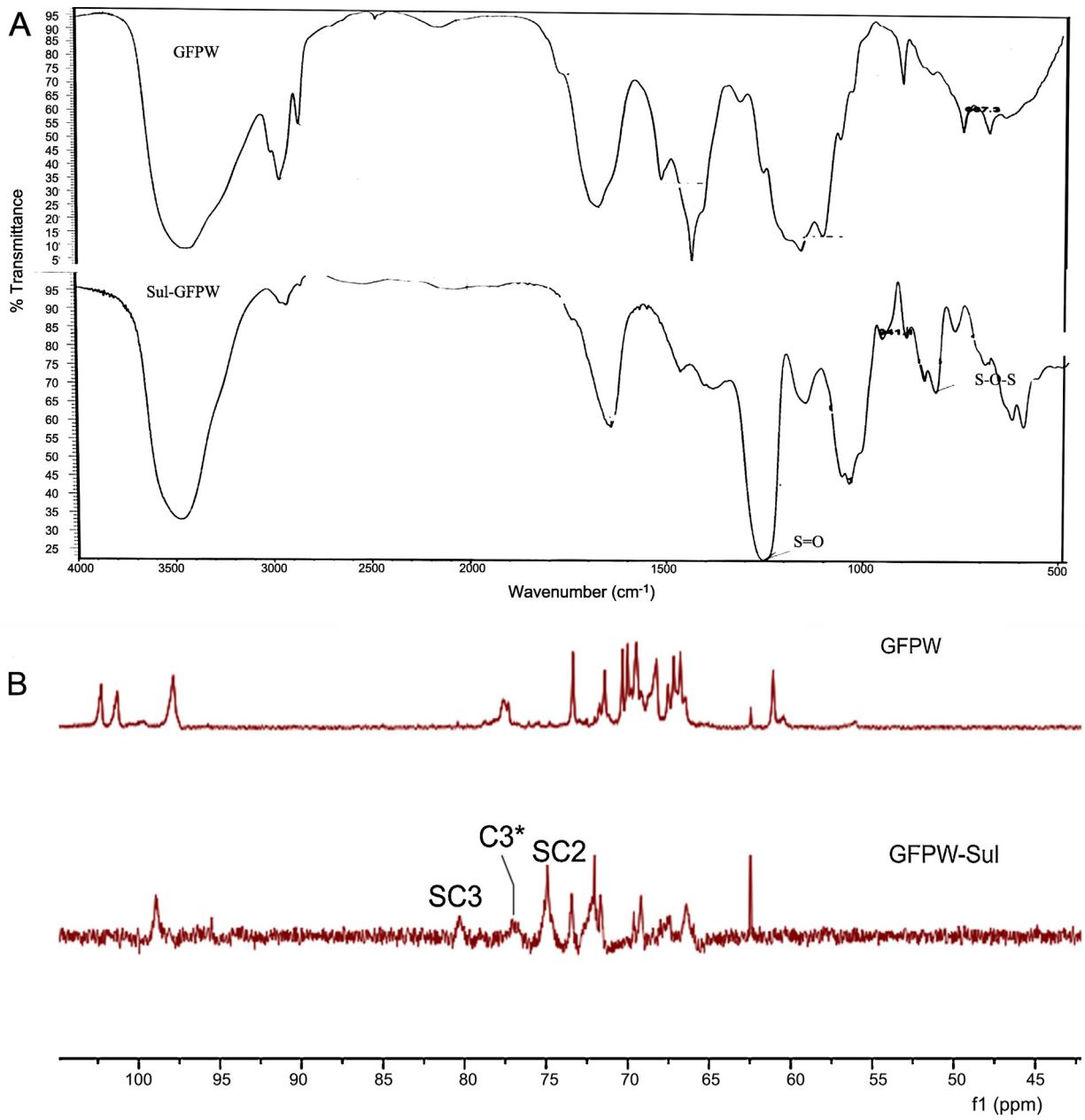

Fig. 4. IR and ^{13}C NMR spectrum of GFPW and Sul-GFPW. (A) IR spectrum of GFPW and Sul-GFPW. (B) ^{13}C NMR spectrum of GFPW and Sul-GFPW.

2011). Meanwhile, other carbon signals in the range of 66–80 ppm could not be assigned without any suspicions because of the serious overlapped. The $[\alpha]_D$ +36° of Sul-GFPW, in comparison with that of GFPW +72°, also implicated a remarkable change in structure due to the sulfation (Table 3). This data was also consistent with that from IR spectrum.

Table 3
Molecular weight, degree of substitution (DS) and specific rotation $[\alpha]_D$ (c 0.05, H_2O) of GFPW and its sulfated derivative Sul-GFPW.

Samples	Molecular weight (kDa)	$[\alpha]_D$ (c 0.05, H_2O)	DS[a]
GFPW	15.7	+72	0
Sul-GFPW	9	+36	0.33

[a] DS is calculated as $162 \times \%W/(96 - 80 \times \%W)$; %W is content of SO_4^{2-}.

3.7. *In vitro antiangiogenesis activities of GFPW and its sulfated derivative*

Angiogenesis is the formation of new capillaries from pre-existing blood vessels which is considered essential for the spread of a tumor, or metastasis. Proliferation and migration of endothelial cells are essential to angiogenesis. To test whether GFPW and its sulfated derivation have any impact on antiangiogenesis *in vitro*, the proliferation effect of GFPW and Sul-GFPW on HMEC-1 cells were evaluated. As shown in Fig. 5A, GFPW did not affect the HMEC-1 cell proliferation, while Sul-GFPW significantly reduced the proliferation of HMEC-1 in a dose-dependent manner when the cells were treated with Sul-GFPW for 72 h. Moreover, HMEC-1 cell proliferation was inhibited by Sul-GFPW at 100 μg/mL in a time-dependent manner (Fig. 5B). To attempt to explain the inhibition of Sul-GFPW on HMEC-1 proliferation, we examined whether Sul-GFPW could modulate cell cycle progression by incubating HMEC-1 with propidium iodide to quantify the percentage of cells in mitogenic phases. Results indicated that Sul-GFPW induced endothelial cells arrested in the S phase (Fig. 5C).

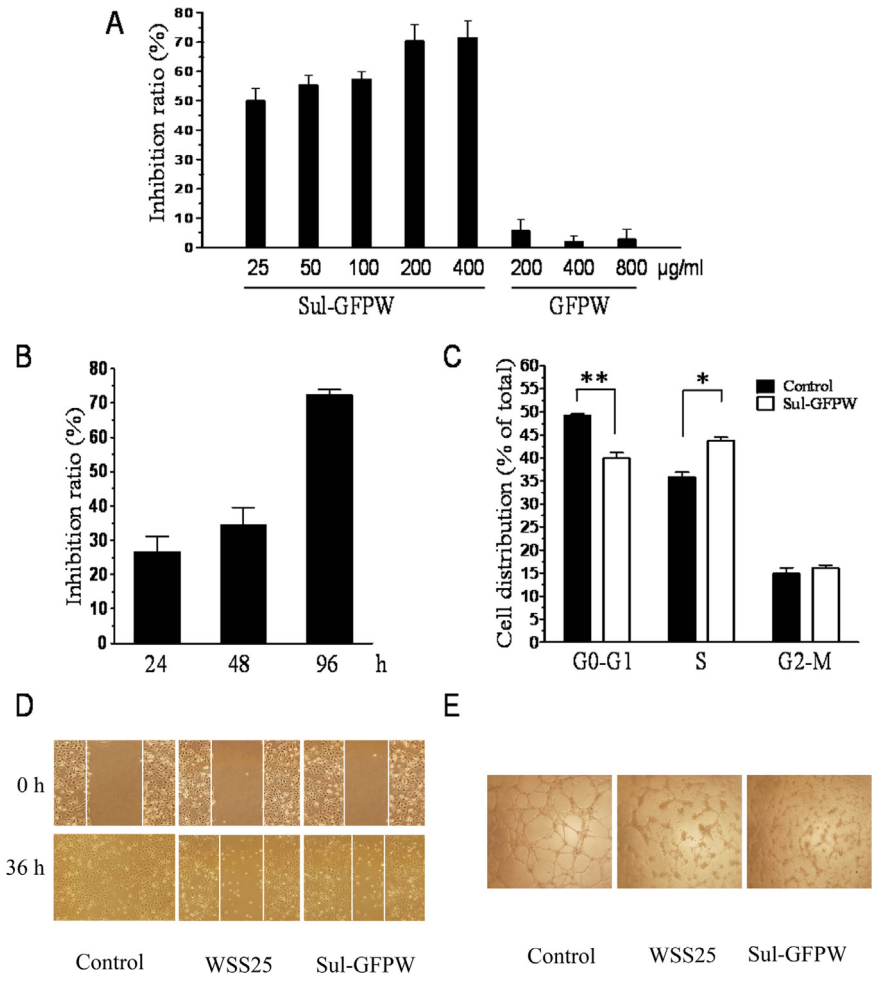

Fig. 5. *In vitro* antiangiogenesis activity of GFPW and sulfated derivative Sul-GFPW. (A) Proliferation effects of GFPW and sulfated derivative Sul-GFPW on HMEC-1 cells. Data were presented as mean ± SD ($n = 5$). (B) Time-dependent effects of Sul-GFPW on the proliferation of HMEC-1. Data were presented as mean ± SD ($n = 5$). (C) Cell cycle analysis of HMEC-1 cells treated with Sul-GFPW for 24 h. Data were presented as mean ± SD ($n = 3$) and indicate the statistically significant at $P < 0.05$ ($^{*}P < 0.05$; $^{**}P < 0.01$). (D) Inhibition effect of WSS25 (25 μg/mL) and Sul-GFPW (100 μg/mL) on HMEC-1 cell migration. (E), WSS25 (25 μg/mL) and Sul-GFPW (100 μg/mL) stunted the capillary-like structures formation of HMEC-1.

Further study showed that Sul-GFPW could also significantly induce the cells apoptosis (Supplementary data Fig. 2), but no necrosis (data not shown). Moreover, we investigated whether Sul-GFPW could inhibit endothelial cell migration. In the presence of Sul-GFPW (100 μg/mL), HMEC-1 migration was significantly decreased compared with the control (Fig. 5D). However, the inhibition effect of Sul-GFPW at the concentration of 100 μg/mL on migration was weaker than that of WSS25 at the concentration of 25 μg/mL. The *in vitro* formation of capillary-like tubes by endothelial cells on a basement membrane matrix is a powerful method to screen for various factors that promote or inhibit angiogenesis. In this study, a tube formation assay of HMEC-1 cells was used to test the angiogenesis activity of Sul-GFPW. HMEC-1 in the control formed a network of tubes within 8 h (Fig. 5E). By contrast, the tube formation was partially inhibited by Sul-GFPW at 100 μg/mL. This effect is similar to that by treatment of WSS25 at 25 μg/mL. These findings support a direct inhibitory effect of Sul-GFPW on endothelial-cell proliferation and migration as well as tube formation *in vitro*. These studies clearly showed that the Sul-GFPW could exhibit antiangiogenesis activity.

Most reports confirmed that polysaccharides exerted their anti-tumor action *via* activation of the immune response of the host organism, or direct by damaging the tumor cells (Chen, Zhao, Chen, & Li, 2008; Sun, Liang, Zhang, Tong, & Liu, 2009; Sun & Liu, 2009; Tong et al., 2009; Wang et al., 2008). Meanwhile, in the past few years, studies related with the effects of polysaccharides on the angiogenesis have increased. A homogalacturonan from the radix of *Platycodon grandiflorum*, PGA4-3b showed negative effect on tube formation, while its degradation derived 4-3bd-O1 and 4-3bde-O2 have anti-angiogenesis activity (Xu, Dong, Qiu, Ma, & Ding, 2011). Polysaccharides from different sources have different antiangiogenesis activities *in vitro*, which depend on their monosaccharide composition, protein content, molecular weight, and chain conformation. Natural sulfated galactans (SGs) are found in marine organism, which exhibit potential pharmacological actions in mammalian systems, such as inflammation, hemostasis, vascular biology, and cancer. Generally speaking, the activity against the neovascularization process performed by the SGs rely on their specific abilities to interfere in the necessary binding properties of some angiogenic factors, mainly the vascular endothelial growth factors (VEGFs) (Cumashi et al., 2007; Koyanagi, Tanigawa, Nakagawa, Soeda, & Shimeno, 2003). A water-soluble polysaccharide, PGAW1, which was isolated from radix of *Platycodon grandiflorum*, was a β-1,4 and β-1,6-linked galactan. Its sulfated derivation could inhibit tube formation in a dose-dependent manner (Xu, Dong, Qiu, Cong, & Ding, 2010). In this study, Sul-GFPW had more obvious inhibitory activity on the growth of HMEC-1 *in vitro* than GFPW at the same concentration and could significantly inhibit HMEC-1 growth in a dose- and time-dependent manner. Preparation of sulfated polysaccharide

derivatives may represent an effective approach for antiangiogenic agents development.

4. Conclusions

In summary, the present study showed that the polysaccharide GFPW from *G. frondosa* was a neutral polysaccharide with an average molecular weight of 15.7 kDa and had a backbone of α-1,6-linked galactopyranosyl residues, with branches attached to O-2, of α-1,3-linked fucose residues and terminal mannose. Bioactivity tests showed sulfated derivative of GFPW named Sul-GFPW significantly reduced the proliferation of HMEC-1 in a dose- and time-dependent manner. Sul-GFPW also could inhibit HMEC-1 migration as well as tube formation *in vitro*. Thus, Sul-GFPW may be a very promising candidate for further development as an antiangiogenic agent.

Acknowledgements

This work was supported by grants from National Natural Science Foundation of China (81171914, 31230022 and 81202103), National Science Fund for Distinguished Young Scholars in China (81125025), New Drug Creation and Manufacturing Program (2012ZX09301001-003), and Industry-University-Research Institute Alliance Fund in Guangdong Province, China (2010A090200041).

Appendix A. Supplementary data

Supplementary data associated with this article can be found, in the online version, at http://dx.doi.org/10.1016/j.carbpol.2013.09.085.

References

Azzam, N. (2007). Angiogenesis and inflammatory bowel disease. *Saudi Journal of Gastroenterology*, *13*(1), 37–38.

Bao, X., Fang, J., & Li, X. (2001). Structural characterization and immunomodulating activity of a complex glucan from spores of *Ganoderma lucidum*. *Bioscience, Biotechnology, and Biochemistry*, *65*(11), 2384–2391.

Bock, K., Pedersen, C., & Pedersen, H. (1984). Carbon-13 nuclear magnetic resonance data for oligosaccharides. In R. S. Tipson, & H. Derek (Eds.), *Advances in carbohydrate chemistry and biochemistry* (vol. 42) (pp. 193–225). Academic Press.

Carmeliet, P. (2003). Angiogenesis in health and disease. *Nature Medicine*, *9*(6), 653–660.

Chen, W., Zhao, Z., Chen, S. F., & Li, Y. Q. (2008). Optimization for the production of exopolysaccharide from *Fomes fomentarius* in submerged culture and its antitumor effect *in vitro*. *Bioresource Technology*, *99*(8), 3187–3194.

Chen, X., Cao, D. X., Zhou, L., Jin, H. Y., Dong, Q., Yao, J., et al. (2011). Structure of a polysaccharide from *Gastrodia elata* Bl., and oligosaccharides prepared thereof with anti-pancreatic cancer cell growth activities. *Carbohydrate Polymers*, *86*(3), 1300–1305.

Cole, C. L., & Jayson, G. C. (2008). Oligosaccharides as anti-angiogenic agents. *Expert Opinion on Biological Therapy*, *8*(3), 351–362.

Cui, F. J., Tao, W. Y., Xu, Z. H., Guo, W. J., Xu, H. Y., Ao, Z. H., et al. (2007). Structural analysis of anti-tumor heteropolysaccharide GFPS1b from the cultured mycelia of *Grifola frondosa* GF9801. *Bioresource Technology*, *98*(2), 395–401.

Cui, H. X., Liu, Q., Tao, Y. Z., Zhang, H. F., Zhang, L., & Ding, K. (2008). Structure and chain conformation of a (1→6)-alpha-D-glucan from the root of *Pueraria lobata* (Willd.) Ohwi and the antioxidant activity of its sulfated derivative. *Carbohydrate Polymers*, *74*(4), 771–778.

Cumashi, A., Ushakova, N. A., Preobrazhenskaya, M. E., D'Incecco, A., Piccoli, A., Totani, L., et al. (2007). A comparative study of the anti-inflammatory, anticoagulant, antiangiogenic, and antiadhesive activities of nine different fucoidans from brown seaweeds. *Glycobiology*, *17*(5), 541–552.

Dodgson, K. S., & Price, R. G. (1962). A note on the determination of the ester sulphate content of sulphated polysaccharides. *Biochemical Journal*, *84*, 106–110.

Fan, J., Zhang, J., Tang, Q., Liu, Y., Zhang, A., & Pan, Y. (2006). Structural elucidation of a neutral fucogalactan from the mycelium of *Coprinus comatus*. *Carbohydrate Research*, *341*(9), 1130–1134.

Harding, L. P., Marshall, V. M., Hernandez, Y., Gu, Y. C., Maqsood, M., McLay, N., et al. (2005). Structural characterisation of a highly branched exopolysaccharide produced by *Lactobacillus delbrueckii* subsp bulgaricus NCFB2074. *Carbohydrate Research*, *340*(6), 1107–1111.

Held, M. A., Be, E., Zemelis, S., Withers, S., Wilkerson, C., & Brandizzi, F. (2011). CGR3: A Golgi-localized protein influencing homogalacturonan methylesterification. *Molecular Plant*, *4*(5), 832–844.

Hoffman, R., Paper, D. H., Donaldson, J., & Vogl, H. (1996). Inhibition of angiogenesis and murine tumour growth by laminarin sulphate. *British Journal of Cancer*, *73*(10), 1183–1186.

Inoue, K., Kohno, M., & Kadoya, S. (1983). Structure-antitumor activity relationship of a D-manno-D-glucan from microellobosporia-grisea – Effect of periodate modification on antitumor-activity. *Carbohydrate Research*, *123*(2), 305–314.

Inoue, K., Nakajima, H., Kohno, M., Ohshima, M., Kadoya, S., Takahashi, K., et al. (1983). An anti-tumor polysaccharide produced by microellobosporia-grisea – Preparation, general characterization, and anti-tumor activity. *Carbohydrate Research*, *114*(1), 164–168.

Kannagi, R., Izawa, M., Koike, T., Miyazaki, K., & Kimura, N. (2004). Carbohydrate-mediated cell adhesion in cancer metastasis and angiogenesis. *Cancer Science*, *95*(5), 377–384.

Kodama, N., Murata, Y., Asakawa, A., Inui, A., Hayashi, M., Sakai, N., et al. (2005). Maitake D-Fraction enhances antitumor effects and reduces immunosuppression by mitomycin-C in tumor-bearing mice. *Nutrition*, *21*(5), 624–629.

Koyanagi, S., Tanigawa, N., Nakagawa, H., Soeda, S., & Shimeno, H. (2003). Oversulfation of fucoidan enhances its anti-angiogenic and antitumor activities. *Biochemical Pharmacology*, *65*(2), 173–179.

Kubo, K., Aoki, H., & Nanba, H. (1994). Anti-diabetic activity present in the fruit body of *Grifola frondosa* (Maitake). I. *Biological and Pharmaceutical Bulletin*, *17*(8), 1106–1110.

Kubo, K., & Nanba, H. (1997). Anti-hyperliposis effect of maitake fruit body (*Grifola frondosa*). I. *Biological and Pharmaceutical Bulletin*, *20*(7), 781–785.

Lee, J. S., Park, B. C., Ko, Y. J., Choi, M. K., Choi, H. G., Yong, C. S., et al. (2008). *Grifola frondosa* (maitake mushroom) water extract inhibits vascular endothelial growth factor-induced angiogenesis through inhibition of reactive oxygen species and extracellular signal-regulated kinase phosphorylation. *Journal of Medicinal Food*, *11*(4), 643–651.

Masuda, Y., Inoue, M., Miyata, A., Mizuno, S., & Nanba, H. (2009). Maitake beta-glucan enhances therapeutic effect and reduces myelosupression and nephrotoxicity of cisplatin in mice. *International Immunopharmacology*, *9*(5), 620–626.

Masuda, Y., Murata, Y., Hayashi, M., & Nanba, H. (2008). Inhibitory effect of MD-Fraction on tumor metastasis: Involvement of NK cell activation and suppression of intercellular adhesion molecule (ICAM)-1 expression in lung vascular endothelial cells. *Biological and Pharmaceutical Bulletin*, *31*(6), 1104–1108.

Miao, Y. S., Li, H. Y., Shen, J. B., Wang, J. Q., & Jiang, L. W. (2011). QUASIMODO 3 (QUA3) is a putative homogalacturonan methyltransferase regulating cell wall biosynthesis in Arabidopsis suspension-cultured cells. *Journal of Experimental Botany*, *62*(14), 5063–5078.

Molinaro, A., Piscopo, V., Lanzetta, R., & Parrilli, M. (2002). Structural determination of the complex exopolysaccharide from the virulent strain of *Cryphonectria parasitica*. *Carbohydrate Research*, *337*(19), 1707–1713.

Nakajima, H., Hashimoto, S., Kita, Y., Takashi, T., Tsukada, W., Kohno, M., et al. (1983). Combination therapy of murine tumors with a degraded D-manno-D-glucan (Dmg) from microellobosporia-grisea, and cyclophosphamide. *Japanese Journal of Experimental Medicine*, *53*(6), 263–269.

Needs, P. W., & Selvendran, R. R. (1993). Avoiding oxidative-degradation during sodium-hydroxide methyl iodide-mediated carbohydrate methylation in dimethyl-sulfoxide. *Carbohydrate Research*, *245*(1), 1–10.

Ohno, N., Asada, N., Adachi, Y., & Yadomae, T. (1995). Enhancement of LPS triggered TNF-alpha (tumor necrosis factor-alpha) production by (1→3)-beta-D-glucans in mice. *Biological and Pharmaceutical Bulletin*, *18*(1), 126–133.

Ohno, N., Suzuki, I., Oikawa, S., Sato, K., Miyazaki, T., & Yadomae, T. (1984). Antitumor activity and structural characterization of glucans extracted from cultured fruit bodies of *Grifola frondosa*. *Chemical and Pharmaceutical Bulletin*, *32*(3), 1142–1151.

Perepelov, A. V., Liu, B., Senchenkova, S. N., Shashkov, A. S., Feng, L., Knirel, Y. A., et al. (2007). Close relation of the O-polysaccharide structure of *Escherichia coli* O168 and revised structure of the O-polysaccharide of *Shigella dysenteriae* type 4. *Carbohydrate Research*, *342*(17), 2676–2681.

Qiu, H., Yang, B., Pei, Z. C., Zhang, Z., & Ding, K. (2010). WSS25 inhibits growth of xenografted hepatocellular cancer cells in nude mice by disrupting angiogenesis via blocking bone morphogenetic protein (BMP)/Smad/Id1 signaling. *Journal of Biological Chemistry*, *285*(42), 32638–32646.

Shen, X., Fang, J., Lv, X., Pei, Z., Wang, Y., Jiang, S., et al. (2011). Heparin impairs angiogenesis through inhibition of microRNA-10b. *Journal of Biological Chemistry*, *286*(30), 26616–26627.

Shih, I. L., Chou, B. W., Chen, C. C., Wu, J. Y., & Hsieh, C. (2008). Study of mycelial growth and bioactive polysaccharide production in batch and fed-batch culture of *Grifola frondosa*. *Bioresource Technology*, *99*(4), 785–793.

Shomori, K., Yamamoto, M., Arifuku, I., Teramachi, K., & Ito, H. (2009). Antitumor effects of a water-soluble extract from Maitake (*Grifola frondosa*) on human gastric cancer cell lines. *Oncology Reports*, *22*(3), 615–620.

Sun, Y., Liang, H., Zhang, X., Tong, H., & Liu, J. (2009). Structural elucidation and immunological activity of a polysaccharide from the fruiting body of *Armillaria mellea*. *Bioresource Technology*, *100*(5), 1860–1863.

Sun, Y., & Liu, J. (2009). Purification, structure and immunobiological activity of a water-soluble polysaccharide from the fruiting body of *Pleurotus ostreatus*. *Bioresource Technology*, *100*(2), 983–986.

Tong, H., Xia, F., Feng, K., Sun, G., Gao, X., Sun, L., et al. (2009). Structural characterization and *in vitro* antitumor activity of a novel polysaccharide isolated from the fruiting bodies of *Pleurotus ostreatus*. *Bioresource Technology*, *100*(4), 1682–1686.

Ulbricht, C., Weissner, W., Basch, E., Giese, N., Hammerness, P., Rusie-Seamon, E., et al. (2009). Maitake mushroom (*Grifola frondosa*): Systematic review by the natural standard research collaboration. *Journal of the Society for Integrative Oncology*, *7*(2), 66–72.

Vaishnav, V. V., Bacon, B. E., O'Neill, M., & Cherniak, R. (1998). Structural characterization of the galactoxylomannan of *Cryptococcus neoformans* Cap67. *Carbohydrate Research*, *306*(1-2), 315–330.

Vinogradov, E., & Wasser, S. P. (2005). The structure of a polysaccharide isolated from *Inonotus levis* P. Karst. mushroom (Heterobasidiomycetes). *Carbohydrate Research*, *340*(18), 2821–2825.

Wang, S. L., Lin, H. T., Liang, T. W., Chen, Y. J., Yen, Y. H., & Guo, S. P. (2008). Reclamation of chitinous materials by bromelain for the preparation of antitumor and antifungal materials. *Bioresource Technology*, *99*(10), 4386–4393.

Xu, Y., Dong, Q., Qiu, H., Cong, R., & Ding, K. (2010). Structural characterization of an arabinogalactan from *Platycodon grandiflorum* roots and antiangiogenic activity of its sulfated derivative. *Biomacromolecules*, *11*(10), 2558–2566.

Xu, Y. X., Dong, Q., Qiu, H., Ma, C. W., & Ding, K. (2011). A homogalacturonan from the radix of *Platycodon grandiflorum* and the anti-angiogenesis activity of poly-/oligogalacturonic acids derived therefrom. *Carbohydrate Research*, *346*(13), 1930–1936.

Ye, L., Zhang, J., Ye, X., Tang, Q., Liu, Y., Gong, C., et al. (2008). Structural elucidation of the polysaccharide moiety of a glycopeptide (GLPCW-II) from *Ganoderma lucidum* fruiting bodies. *Carbohydrate Research*, *343*(4), 746–752.